ChemComm
Chemical Communications

Accepted Manuscript

This article can be cited before page numbers have been issued, to do this please use: A. Srivastava, P. Jain, G. Gadikota, P. Ochonma, C. Noe and T. Yin, *Chem. Commun.*, 2024, DOI: 10.1039/D4CC04632C.

ROYAL SOCIETY OF CHEMISTRY

rsc.li/chemcomm

ChemComm

View Article Online
DOI: 10.1039/D4CC04632C

COMMUNICATION

Separation of Rare Earth Elements and Nickel Harnessing Electrochemistry and Reactive CO_2 Capture and Mineralization

Received 00th January 20xx,
Accepted 00th January 20xx

DOI: 10.1039/x0xx00000x

Prince Ochonma,[a] Akanksha Srivastava,[b] Christopher Noe,[c] Tianhe Yin,[b] Prarabdh Jain,[a] and Greeshma Gadikota[a,b,*]

The aim is to probe the chemical mechanisms underlying the use of multifunctional solvents to simultaneously capture and convert CO_2 into insoluble Rare Earth Element (REE)-carbonates, while forming soluble complexes with nickel for separation. Subsequent nickel electrodeposition regenerates the CO_2-loaded solvent for reuse.

Advances in technologies that harness CO_2 emissions for the recovery of energy relevant metals are needed to accelerate the energy transition for a stable climate future.[1] In particular, the energy transition has led to a significant increase in the demand for critical metals such as REEs and nickel, challenged by their limited supply due to uneven geographic distribution or geologic scarcity and the rapid depletion of conventional high grade ores.[2] These challenges have led to scientific interest in metal recovery from unconventional sources such as industrial residues[3] and recycled materials.[4] Industrial facilities are being developed for metal separations using pyrometallurgy or the use of heat to extract metals[5] and hydrometallurgy which involves leaching using chemically consumptive reagents and liquid - liquid extraction for separation.[6–8] Despite significant progress, the greenhouse gas footprint associated with heating, or the use of these reagents is significant,[9] and alternative environmentally sustainable pathways are needed for the recovery and separation of these metals. One of the less explored but highly transformative pathways to decarbonize the recovery and separation of metals involves the capture and use of CO_2. Metal chelating amine ligands such as ethylenediaminetetraacetic acid (EDTA) has been demonstrated for simultaneous CO_2 mineralization and recovery of metals such as Ni, Fe, and Cr in the solution phase.[10] However, the use of CO_2 capture solvents for the separation of REEs and transition metals such as Ni remains less explored.

In this context, it is well – known that the REE – carbonates have low solubilities in water and can be preferentially separated via crystallization using CO_2 capture solvents that solubilize CO_2 and are regenerated on the precipitation of REE – carbonates. The separation of La, Ni, and Co was reported using diethylenetriamine and carbon dioxide - bearing flue gas.[4] After the precipitation of lanthanum carbonate, subsequent separations were realized using ethanol and CO_2 to separate Ni^{2+} and Co^{2+} ions. While this separation pathway is effective, this approach uses multiple solvent-based techniques for sequential separation and efficient solvent regeneration is essential to realize favourable economics. An alternative approach would be to utilize multifunctional solvents that can effectively capture CO_2, precipitate REE-carbonates, and serve as an effective medium for Ni precipitation without undergoing degradation. This approach eliminates the need for additional solvents for Ni recovery and instead regenerates the multifunctional solvent which can be looped multiple times for separating REEs (La^{3+}, Pr^{3+}, Nd^{3+}, Eu^{3+}, Dy^{3+}) ions from Ni^{2+} ions.

These scientific possibilities and challenges motivate the investigation of CO_2 capture solvents such as aqueous ammonium hydroxide (NH_4OH), aqueous monoethanolamine (MEA), and aqueous diethylenetriamine (DETA). NH_4OH was chosen given its effectiveness in forming soluble complexes with Ni.[11] MEA has been shown to be effective in capturing and converting CO_2 to REE-carbonates.[12] DETA has been reported for separating La and Ni in solvent – based extraction[4] though its effectiveness for electroplating is unexplored. Despite these advances, the following specific research questions remain unexplored: **(1)** What are the chemical mechanisms associated with the use of amine bearing CO_2 capture solvents for REE and Ni separations? **(2)** After the recovery of REE-carbonates, what is the efficacy and associated coulombic efficiencies of Ni electrodeposition? **(3)** What is the influence of chemical speciation on product yields, purities, and morphologies? Addressing these questions will unlock new insights into the multifunctional role of solvents in capturing CO_2, enabling the separation of REEs as water – insoluble carbonates, and mediating Ni electrodeposition (see **Fig. 1**).

To elucidate the importance of CO_2 capture solvents in enhancing CO_2 solubility, and facilitating REE separation, two control experiments are conducted with solutions bearing 588 ppm La and 1176 ppm Ni. In the first control experiment, CO_2 is bubbled directly through the aqueous La/Ni solution for 12 hours resulting in no precipitation. Consequently, no carbonate

[a] *Smith School of Chemical and Biomolecular Engineering, Cornell University, Ithaca, NY 14853*
[b] *School of Civil and Environmental Engineering, Cornell University, Ithaca, NY 14853*
[c] *Department of Chemistry, College of Art and Science, Stony Brook University, Stony Brook, NY 11790*
Supplementary Information available: [details of any supplementary information available should be included here]. See DOI: 10.1039/x0xx00000x

View Article Online
DOI: 10.1039/D4CC04632C

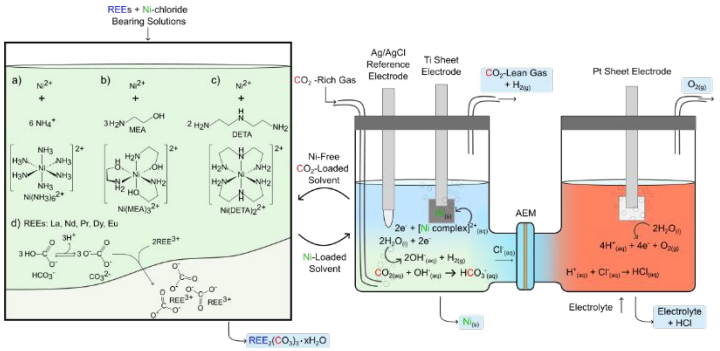

Fig. 1. Schematic representation of the proposed approach to separate La and Ni by harnessing CO_2 using metal chelating multifunctional CO_2 capture solvents. Preferred reactions (based on stability of complexes shown in **S.I Table 2**) in the solution phase are illustrated with **(a)** ammonium hydroxide (NH_4OH), **(b)** monoethanolamine (MEA) and **(c)** diethylenetriamine (DETA). Potential products that could be obtained from this process include REE-carbonates, electrodeposited nickel, H_2 and O_2, while the solvent is regenerated for the subsequent cycle. All measurements are performed at room temperature.

formation is observed due to the low solubility of CO_2 in pure water, indicating that CO_2 capture solvents are needed. In the second control experiment, equal volumes of CO_2 loaded aqueous NaOH, and aqueous La/Ni solution are mixed, which resulted in La recovery efficiencies as lanthanum carbonate up to 99.9 (± 0.1) %. However, this is also accompanied by 70.7% (± 0.5) % of Ni precipitation resulting in La-carbonate purity and separation factor (β) of 46.4 (± 0.7) % and 370.5 (± 8.2), respectively. These base case separation factors are within a similar range of 314.6 – 3827.8 for La/Ni separation reported using other separation processes.[6–8] Nonetheless, more selective separation of La and Ni can be achieved by co-utilizing CO_2 and soluble metal chelating agents, which motivated the investigation of NH_4OH, MEA, and DETA.

As shown in **Fig. 2** and **Table S.1**, La recovery efficiencies exceeding 99.5% is reported with NH_4OH, MEA, and DETA. In addition, suppressed Ni co-extraction is observed (0 – 17.53% co-recovery efficiencies) at similar conditions with the control experiments (1:2 for La: Ni) resulting in separation factors of (4524 – 11630), (2131 – 4457), and (8784 – no Ni detected in carbonate phase) for NH_4OH, MEA, and DETA, respectively. Increasing Ni co-extraction efficiency is reported in the order of DETA < NH_4OH < MEA. Notably, this trend in Ni co-extraction efficiency is significantly influenced by the ability for Ni to form stable complexes in solution. **Table S.2** shows that Ni-DETA complexes have higher stabilities compared to those with NH_4OH or MEA. The formation of this soluble complex is also evident from the change in the colour of the solution bearing Ni

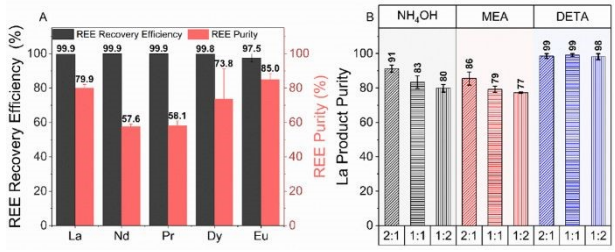

Fig. 2. (a) Recovery efficiencies and product purity for REE/Ni separation using NH_4OH at REE:Ni of 1:2. **(b)** The product purity at different concentration ratios for NH_4OH, MEA and DETA.

from green to purple on DETA addition (**Fig. S.1 (d)**). The effectiveness of harnessing NH_4OH for separating other REEs such as Praseodymium (Pr), Neodymium (Nd), Europium (Eu), and Dysprosium (Dy) is also investigated. From a thermodynamic standpoint, the respective stability constants of REE – carbonates are similar, which is an indicator of similar behaviour as with La while keeping all other factors constant. **Fig. 2 (a)** and **Table S.1** also show that recoveries exceeding 98% are also observed for all the four REEs of interest. Moreover, the regeneration of the CO_2-free solvent can be achieved at higher REE concentrations as demonstrated with MEA in **Fig. S.2 a-d**.

Evidence of REE carbonate formation is determined by investigating the thermal decomposition behaviour using TGA (**Fig. S.3).** Weight losses in the range of 80 – 240 ºC accounts for ~6.7 %, 7.2 % and 5.7 % of the sample weight in NH_4OH, MEA and DETA respectively are associated with the loss of H_2O molecules implying the presence of hydrated carbonate species.[13,14] Higher loss of H_2O observed with MEA and NH_4OH is likely due to the presence of hydrated Ni-carbonate. This observation is confirmed by the weight loss in the temperature range of 210 – 430ºC associated with the loss of CO_2 in Ni-carbonate.[14] **Fig. S.4 (a)** shows the TGA, DTG and DSC profile of pure hydrated Ni- carbonate for comparison. It is important to note that Ni-hydroxide and Ni-carbonate decompose at overlapping temperature ranges.[14] However, FTIR confirm the absence of the characteristic OH stretching vibrations of $Ni(OH)_2$ typically observed at 3645 (± 3) cm^{-1} [15] as shown in **Fig. S.4 (b).** In the next step, at temperatures in the range of 260 °C - 580 ºC, lanthanum carbonate $La_2(CO_3)_3$ decomposes into $La_2O_2(CO_3)$, releasing CO_2.[13] The fourth weight loss is perhaps the most distinct characteristic weight loss feature of lanthanum carbonate which represents the decomposition of $La_2O_2CO_3$ to release CO_2 and produces La_2O_3.[13] DETA is observed to have the highest weight loss (~7%) compared with ~4% in MEA and NH_4OH implying a relatively higher purity of La-carbonate. This observation is further confirmed by the distinct green colour of Ni in the final product recovered from experiments performed using NH_4OH and MEA (**Fig. S.5**) contrasted with a product free of any coloration obtained from DETA post separation. SEM images shown in **Fig. S.3 (d-f)** reveal the presence of aggregated clusters with rosette and flat morphologies in all lanthanum carbonate samples produced.

Cathodic Reactions

$Ni(NH_3)_6Cl_{2(aq)} + 2e^- \rightarrow Ni_{(s)} + 6NH_{3(aq)} + 2Cl^-_{(aq)}$ E^0 = -0.48V(*vs* SHE) (R1)[16]

$Ni(H_2NC_2H_4OH)_3Cl_{2(aq)} + 2e^- \rightarrow Ni_{(s)} + 3H_2NC_2H_4OH_{(aq)} + 2Cl^-_{(aq)}$ (R2)

$Ni(C_{14}H_{13}N_3)_2Cl_{2(aq)} + 2e^- \rightarrow Ni_{(s)} + 2C_{14}H_{13}N_{3(aq)} + 2Cl^-_{(aq)}$ (R3)

$2H_2O_{(aq)} + 2e^- \rightarrow 2OH^-_{(aq)} + H_{2(g)}$ E^0= -0.41V(vs SHE, pH =7) (R4)[16]

$OH^-_{(aq)} + CO_{2(g)} \rightarrow HCO_3^-{}_{(aq)}$ (R5)[10]

$OH^-_{(aq)} + HCO_3^-{}_{(aq)} \rightarrow CO_3^{2-}{}_{(aq)} + H_2O$ (R6)[17]

Anodic Reactions

$H_2O_{(aq)} \rightarrow 2H^+_{(aq)} + 1/2O_{2(g)} + 2e^-$ $E^0 = 0.82V$ (vs SHE, pH =7) (R7)[3]

$H^+_{(aq)} + Cl^-_{(aq)} \rightarrow HCl_{(aq)}$ (R8)[18]

The reactions proposed for Ni recovery are shown in **R1–R8**. Ni deposition at the cathode is facilitated by decomplexation through a gain of electrons to deposit solid Ni species as shown in **R1–R3**. Thermodynamic plots shown in **Fig. S.6** show the possibility for Ni to form complexes of varying oxidation states including $[Ni(NH_3)_x]^{2+}$, $[Ni(H_2NC_2H_4OH)_x]^{2+}$, and $[Ni(C_{14}H_{13}N_3)_x]^{2+}$, where x typically varies from 1–6, 1–3, and 1–2 in NH_4OH, MEA, and DETA, respectively. Nonetheless, complexes discussed in this study and represented in **R1–R3** are the most stable reported Ni-complexes with NH_4OH, MEA or DETA where x is 6, 3 and 2 respectively (**See Table S.2**). One important side reaction to consider is the hydrogen evolution reaction (HER) which occurs at the cathode and competes for electrons as shown in **R4**. HER requires a similar number of electrons as Ni electrodeposition which implies that neither has a kinetic advantage. However, HER is more favoured to occur at higher potentials, and at lower Ni concentrations,[19] due to rapidly depleting supersaturation around the electrode surface leading to lower Ni electrodeposition Coulombic efficiencies (CE).[16]

To evaluate the effect of NH_4OH, MEA, and DETA on the electrochemical reduction of Ni, linear sweep voltammetry (LSV) curves are obtained in **Fig. S.7**. We observe two significant differences in the LSV curves for all the three solvents investigated. First, the overpotentials required for Ni reduction are observed to be lower for NH_4OH (-0.454 V vs RHE) and MEA (-0.496 V vs RHE) compared with DETA (-0.638 V vs RHE). The lower reduction potential values obtained with DETA are in fact due to the formation of a more stable Ni complexes with DETA compared to NH_4OH and MEA. Thus, a higher overpotential is required for Ni deposition. Despite the slightly lower stability of Ni complexes with MEA compared with NH_4OH, higher

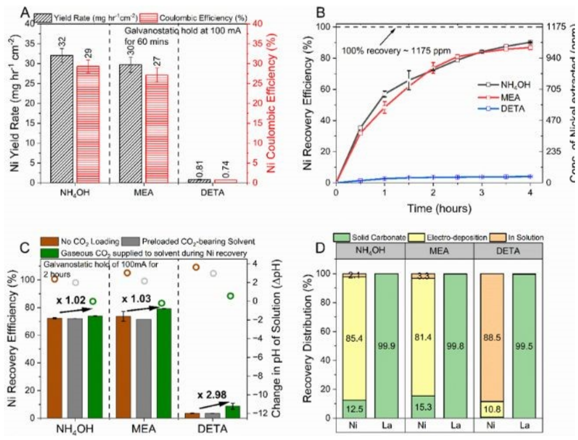

Fig. 3 (a).Ni yield rate and coulombic efficiencies in different CO_2 capture solvents at galvanostatic hold of 100 mA for 1 hr. **b)** Comparison of Ni recovery efficiency as a function of time for NH_4OH, MEA and DETA **c)** The effect of CO_2 loading on Ni recovery efficiency. **d)** Integrated experiments showing distribution of products as carbonates, electrodeposition material and unrecovered metal.

reduction potential with MEA is reported. We hypothesize that this could be due to slower rates of charge transfer because of lower ion mobility with Ni-MEA complex compared to Ni-NH_3 due to the larger ionic size. The second observation is that the slopes of the LSV curves in **Fig. S.7** decrease in the following order: NH_4OH > MEA > DETA. This decrease in slope has been reported to be due to decreased mass transfer of Ni towards the surface of the electrode.[11]

Since regeneration of the impurity-free CO_2 loaded solvent is of importance, it is essential that these reactions are carried out in a two-chamber cell to facilitate the migration of Cl^- ions. It has been reported that the chlorine evolution reactions could occur in a one-chamber cell at the anode leading to the evolution of chlorine gas.[16] Moreover the formation of Cl_2 gas could result in a homogenous reaction with NH_3 to produce N_2 leading to ammonia consumption.[11] Ammonia consumption through this reaction has been reported in the order of 0.193 kg of NH_3/kg of Ni.[11] Furthermore, the buildup of Cl^- ions could lead to increased acidity and solvent degradation. These side reactions can be avoided by the proposed two chamber cell configuration with an AEM to facilitate the migration of Cl- ions to the anode. At the anode, oxygen evolution reaction (OER) occurs producing protons that stabilize the Cl- ions to generate HCl as shown in **R7 - R8**.

Fig. 3 (a) shows the (CE) and the yield rate of Ni per unit area of titanium electrode for each solvent at a galvanostatic hold of 100 mA for 1 hour. The highest yield rates and CE of 32 mg hr^{-1} cm^{-1} and 29 % respectively are both obtained with NH_4OH. The CE and rate of deposition of these systems is dependent on the starting concentration of Ni and the electrolyte.[19] CE of 45% have been reported for electrodeposition of 1,700 ppm Ni from a single chamber cell in an ammoniacal buffer system consisting of $(NH_4)_2SO_4$, NH_3 and H_2SO_4.[16] Moreover the CE is observed to slowly decrease with time **(Fig. S.8)**, which matches the asymptotic behaviour also observed with Ni recovery efficiencies as a function of time shown in **Fig. 3 (b)**. Up to 90% of Ni is electrodeposited after 4 hours of electrolysis from NH_4OH and MEA, and up to 4% with DETA. Early asymptotic behaviour is observed with DETA resulting in slower deposition rates. This behaviour is likely due to the transformation of NiDETA complex remaining in solution to the more stable $Ni(DETA)_2$ complex due to an increase in the pH because of competing HER **(Table S.2)**. The change in the solution pH of 3.64 from neutral conditions is observed which implies that $Ni(DETA)_2$ complex becomes more prominent in this system according to thermodynamic speciation calculations shown in **Fig. S.6**, implying that a buffer system is required. A similar slow pH increase is observed with NH_4OH and MEA which is detrimental for electrodeposition as Ni species undergo hydrolysis at higher pH conditions to precipitate as hydroxides.

The pH changes in these systems are typically modulated by the addition of a buffer. Boric acid is widely used to control pH and reduce the overpotential as it forms weak Ni borate complex ($Ni(H_2BO_3)_2$) in solution.[20] Alternatively, we propose the use of CO_2. The dissolution and speciation of CO_2 into carbonate and bicarbonate species typically results in the consumption of OH^- ions produced because of the HER (**R4 – R6**), thus the pH can be controlled. Moreover, CO_2 forms carbamate species with amine species which could also aid in Ni extraction. As shown in **Fig. 3 (c)**, the continuous supply of CO_2 during electrodeposition is found to improve the recovery efficiencies by 1.02, 1.03, and 2.98 times for NH_4OH, MEA and DETA respectively after 120 mins. Further, the change in pH of the solution was observed to be -0.01, -0.21, and 0.57 for NH_4OH, MEA and DETA respectively, compared to 2.37, 3.03, and 3.64 obtained without CO_2. The relatively higher ΔpH of the solution observed with DETA compared to MEA and NH_4OH is also an indication of the lower Ni extraction CE obtained in **Fig. 3 (a)** because of HER. We also observed that the presence of CO_2 significantly influenced Ni electrodeposition through

modulation of pH as opposed to complexation. Experiments performed using preloaded CO_2 solvent post REE separation showed no significant enhancement in Ni recovery, despite NMR analysis confirming the presence of similar amine-CO_2 species such as carbamates, HCO_3/CO_3^{2-} ions **(Fig. S.9)**.

The chemical phases, structural and morphological features of the electrodeposited Ni, is discussed using XRD, SEM and XPS analyses. **Fig. S.10 (a-c)** shows the formation of dark shiny particles on the surface of the electrode indicating a successful electrowinning process. Ni particles of different sizes are observed in **Fig. S.11 (a-f).** The Ni deposit obtained for NH_4OH, MEA, and DETA at galvanostatic hold of 100 mA appeared to be a non-compact, silvery dark powder with spherical morphology which could be easily scraped off the titanium sheet electrode **(Fig. S.11 (a-f))**. It is important to also disclose that a different sheet-like morphology is observed when working at lower current densities < 5 mA (**See Fig. S.12 c**). XRD analysis on the scraped powder showed the presence of 111, 200, and 220 phases in **Fig. S.12** associated with pure metallic Ni (PDF 03-065-2865). This is confirmed by high resolution XPS scans which showed the characteristic binding energy of Ni^0 for $2p^{3/2}$ at 852.7 eV with ΔE of 17.27 from $2p^{1/2}$ indicating the presence of pure metallic Ni. This Ni^0 peak decreased in intensity when comparing NH_4OH to MEA and could not be detected in the Ni species from DETA. XRD analysis on the Ti electrode bearing Ni for DETA confirms the presence of Ni oxides as opposed to pure metallic Ni observed with NH_4OH and MEA.

To illustrate the flexibility of this concept for integrated CO_2 capture and the separation of REEs and Ni, we performed a stepwise separation of La and Ni using CO_2 loaded aqueous NH_4OH, MEA and DETA. Lanthanum carbonate phases with > 99.5% yield in all solvents is observed as shown in **Fig. 3 (d).** However, 12.5% and 15.3% Ni-carbonates are also co-recovered. As discussed earlier, the product purity at this step could be further enhanced by controlling the concentration of CO_2 species in solution. The relatively small difference in $NiCO_{3(aq)}$ and $Ni\text{-}NH_4OH_{(aq)}/Ni\text{-}MEA_{(aq)}$ complexation stability constants implies that a fraction of Ni could precipitate as carbonate product. On the other hand, insignificant quantities of Ni are observed with DETA due to the formation of a significantly stronger complex. This stronger complexation challenges electrochemical Ni recovery in the subsequent step. Ni recovery up to 85 % and 81 % is obtained from the solution post La separation using NH_4OH and MEA. However, only 11% of Ni is recovered using DETA. To increase Ni electrodeposition efficiency, temperature can be increased which enhances electrolyte conductivity, ion diffusivity, and the charge transfer rate leading to lower overpotentials and changes in the redox potential of species. However, the risk of solvent decomposition exists. Alternatively, the synthesis of solvents that binds Ni preferentially over REE at log K values in the range of 10 – 18 can be explored. It is crucial that the binding affinities of Ni ions with the solvent are not too strong which could otherwise prevent Ni electrodeposition. Furthermore, solvents need to be chemically stable and show superior CO_2 capture performance.

In summary, harnessing CO_2 capture solvents for separating rare earth elements (REEs) and Ni is highly effective. REE yields up to 99% are obtained while realizing product purities of 80%, 79% and 98% with NH_4OH, MEA and DETA, respectively. Although DETA is more effective in aiding the separation of REE and nickel the strong Ni-complex formation challenges nickel recovery during electrodeposition. Also, the supply of CO_2 during electrodeposition is effective as CO_2 modulates pH and forms alternative complexes that improves Ni recovery rates. Scalable deployment can be realized by further tuning this approach to maximize H_2 and O_2 recovery and achieving efficient solvent regeneration over multiple cycles.

Cornell Center for Materials Research (CCMR) ((NSF MRSEC) program (DMR-1719875)) is acknowledged. P.O acknowledges the support of the Link Foundation Energy Fellowship. A.S. and G. G. acknowledge the support of Engineering Learning Initiatives and the Sprout Award from Cornell University.

Author contributions

P.O. developed the concept, conducted experiments and characterization and completed the first draft. C. N. supported experiments. C.N and P. J. supported characterization. A. S. and T. Y. conducted the feasibility studies. G.G. conceptualized this work, obtained support, and edited this manuscript.

Data availability

The data supporting this article has been included as part of the ESI.

Conflicts of interest

G.G. co-founded Carbon To Stone to advance industrial decarbonization.

Notes and references

1 Dolf. Gielen, *International Renewable Energy Agency*, 2021.
2 É. Lèbre, J. R. Owen, G. D. Corder, D. Kemp, M. Stringer and R. K. Valenta, *Environ Sci Technol*, 2019, **53**, 10571–10579.
3 P. Ochonma, X. Gao and G. Gadikota, *Acc Chem Res*, 2024, **57**, 267–274.
4 J. Septavaux, C. Tosi, P. Jame, C. Nervi, R. Gobetto and J. Leclaire, *Nat Chem*, 2020, **12**, 202–212.
5 E. G. Polyakov and A. S. Sibilev, *Metallurgist*, 2015, **59**, 368–373.
6 A. Rout and K. Binnemans, *Phys Chem Chem Phys*, 2016, **18**, 16039–16045.
7 A. Rout, S. Wellens and K. Binnemans, *RSC Adv*, 2014, **4**, 5753–5758.
8 S. Satpathy and S. Mishra, *Sep Purif Technol*, 2017, **179**, 513–522.
9 T. Norgate and S. Jahanshahi, *Miner Eng*, 2011, **24**, 1563–1570.
10 S. Katre, P. Ochonma, H. Asgar, A. M. Nair, K. Ravi and G. Gadikota, *Phys Chem Chem Phys*, 2024, **26**, 9264–9283.
11 R. Cruz-Gaona, D. Dreisinger and C. Roel Cruz, *In Electrochemistry in Mineral and Metal Processing VI: Proceedings of the International Symposium*, 2003, **2003**, 304.
12 P. Kim, G. Das, M. M. Lencka, A. Anderko and R. E. Riman, *J Mater Eng Perform*, 2020, **29**, 5564–5573.
13 X. H. Zhang, C. He, L. Wang, Z. Q. Li and Q. Feng, *J Therm Anal Calorim*, 2015, **119**, 1713–1722.
14 M. A. Rhamdhani, E. Jak and P. C. Hayes, *Metall. Mater. Trans. B*, 2008, **39**, 218–233.
15 M. S. Vidhya, G. Ravi, R. Yuvakkumar, D. Velauthapillai, M. Thambidurai, C. Dang and B. Saravanakumar, *RSC Adv*, 2020, **10**, 19410–19418.
16 C. Lupi, M. Pasquali and A. Dell'Era, *Miner Eng*, 2006, **19**, 1246–1250.
17 P. Ochonma, C. Noe, S. Mohammed, A. Mamidala and G. Gadikota, *React Chem Eng*, 2023, **8**, 1943–1959.
18 M. Kim, P. Lu, P. Ochonma and G. Gadikota, *Energ Fuel* 2024, **38**, 15812–15822.
19 T. Tawonezvi, D. Zide, M. Nomnqa, L. Petrik and B. J. Bladergroen, *Chem Eng J Adv*, 2024, **17**, 100579.
20 J. Ji, W. C. Cooper, D. B. Dreisinger and E. Peters, *J Appl Electrochem*, 1995, **25**, 642-6505.

View Article Online
DOI: 10.1039/D4CC04632C

The data supporting this article have been included in the main manuscript and the supplementary information.